Erosion Rate Prediction Model for Levee-Floodwall Overtopping Applications in Fine-Grained Soils

By Parham Safarian Bahri, Bachelor of Science in Civil Engineering

A Thesis Submitted in Partial
Fulfillment of the Requirements
for the Degree of
Master of Science
in the Field of Civil Engineering

Advisory Committee:

Abdolreza Osouli, Chair

Ryan Fries

Rohan Benjankar

Graduate School
Southern Illinois University Edwardsville
May, 2017

ABSTRACT

EROSION RATE PREDICTION MODEL FOR LEVEE-FLOODWALL OVERTOPPING APPLICATIONS IN FINE-GRAINED SOILS

By

Parham Safarian Bahri

Chairperson: Assistant Professor Abdolreza Osouli

Characterizing soil erosion and predicting levee erosion rates for various levee soils and storm conditions during floodwall overtopping events is necessary in designing levee-floodwall systems. In this study, a series of laboratory scaled levee-floodwall erosion tests were conducted to determine erosion characteristics of fine grained soils subject to overtopping from different floodwall heights with variable flow-rates. After the initiation of scouring, a pool of water was created at the levee crest which caused the erosion rate to decrease. The erosion rates were also assessed using Jet Erosion Test (JET) and Erosion Function Apparatus (EFA) tests. The results of levee-floodwall overtopping along with soil geotechnical characteristics such as plasticity index, compaction level, and saturation level of the levee soils as well as hydraulic parameters such as water overtopping velocity were used to develop a levee-floodwall erosion rate Prediction Model. Then, the results of JET and EFA were integrated to develop another Prediction Model for levee-floodwall erosion rate estimation. Consequently, the prediction models were evaluated by conducting additional tests and comparing the prediction results with the actual measured erosion rates.

Keywords: Levees, Overtopping, Floodwall, EFA, JET, Flume Test, Cohesive Soils, Erosion, Scour

ACKNOWLEDGEMENTS

I would like to thank my advisor, Dr. Abdolreza Osouli for his guidance and support during my Master's Thesis process. He showed me the way to conduct this research and provided any means necessary for this project to advance smoothly and effectively. Dr. Osouli's supervision throughout my thesis research helped me find the answers I was looking for by showing me the right path towards the answers not by providing the answer itself which taught me the basics of research work. Furthermore, I would like to express my gratitude to my other thesis committee members, Dr. Ryan Fries and Dr. Benjankar, for their directions and their feedbacks on my thesis. I would also like to thank our Soils Laboratory Specialist, Mr. Brent Vaughn, for his assistance throughout the laboratory phase of this research.

Moreover, I would like to thank Mr. Mazdak Karimpour and Mr. David Molohon for their role in my thesis research progress by helping me run a large number of laboratory tests which included twelve Jet Erosion Tests, over 40 EFA Tests, and 45 Levee-Floodwall Tests. I would also like to express my gratitude to Mr. Sina Nassiri and Mr. Sajjad Salam for their support and assistance during the various phases of the laboratory tests.

Finally, I am grateful to my family who supported every single decision that I have made in my life and always showed me the right path in every stage of my education and my personal life. Without their help and support, I would not be able to be where I am today and I would not be the person I am today.

DISCLAIMER STATEMENT

This dissertation was prepared by Parham Safarian Bahri Master's student at Southern Illinois University Edwardsville under the supervision of Dr. Abdolreza Osouli for academic purposes only. Neither Parham Safarian Bahri, Southern Illinois University Edwardsville, nor any person acting on behalf of either:

(A) Makes any warranty of representation, express or implied, with respect to the accuracy, completeness, or usefulness of the information contained in this report, or that the use of any information, apparatus, method, or process disclosed in this report may not infringe privately-owned rights; or

(B) Assumes any liabilities with respect to the use of, or for damages resulting from the use of, any information, apparatus, method or process disclosed in this report.

Notice to Journalists and Publishers: If you borrow information from any part of this dissertation, you must include author's name and Southern Illinois University Edwardsville Civil Engineering Department.

TABLE OF CONTENTS

LIST OF FIGURES

LIST OF TABLES

LIST OF SYMBOLS

ASTM	American Society for Testing and Materials
EFA	Erosion Function Apparatus
HET	Hole Erosion Test
JET	Jet Erosion Test
SET	Slot Erosion Test
PI	Plasticity Index
CL	Compaction Level, Lean Clay
ML	Low Plastic Silt
SR	Saturation Ratio
$\dot{\varepsilon}$	Erosion Rate

GLOSSARY

Erosion - In geomorphology and geology, erosion is the action of exogenic processes (such as water flow or wind) removing soil and rock from one location and transporting it to another location where it is deposited.

Overtopping – The level of water exceeding the level of the levee

Piping - Internal erosion of the levee which undermines it

Floodwall – The structure placed on the crest of the levee to increase the height of the levee

Erodibility – Material's erosion capability

Nappe – A sheet of water flowing over a levee, dam or similar structure when overtopping is in progress

Shear strength - The capability of levee material to withstand the forces which result in failure in shear

Breach - A breach can be a sudden or gradual failure, caused either by surface erosion or by subsurface weakness in the levee xiv

American Society of Testing and Materials (ASTM) - An international standards institute that produces and issues technological standards regarding an extensive collection of materials, testing guidelines, methods, and facilities

CHAPTER I

INTRODUCTION AND LITERATURE

1.1 Scope and Significance

The scour developed at the levee crest on the landside of the floodwall due to floodwall overtopping results in lack of support for the wall and consequently levee failure. The scour occurs due to the relocation of soil particles with the flow of water (Amini et al. 2013). For coarse-grained soils, the erosion occurs by the relocation of soil particles one by one; however, for fine-grained soils, the erosion occurs by the relocation of each particle or by blocks of particles. There have been many examples of levee failures around the world due to storm events (Baars 2004; Chang et al. 2011; Villarini et al. 2011; Tirpak 2009; Briaud et al. 2008). An understanding of levee material resistance against erosion is the critical information in the design of levees and precautionary actions against levee-floodwall failure.

During storm events, the water level behind the floodwall rises. Overtopping initiates once the water reaches the top of the wall. The overtopped water impinges the levee crest and applies shear stress to the levee surface. Scouring initiates once the applied shear stress exceeds the soil's critical shear stress or resistance. The applied shear stress can be estimated using overtopping velocity (Pan et al. 2015). It is worth noting that this stress can be magnified by turbulence and wave action of the overtopped water (Xiao et al. 2009; Yuan et al. 2015).

1.2 Commonly Practiced Lab and Field Tests

Various field and laboratory tests have been developed for characterizing soil erosion rates or erodibility. The most commonly used tests are Erosion Function Apparatus (i.e. EFA) test (Briaud et al. 2001), Jet Erosion Test (i.e. JET) (ASTM D 5852), Hole and Slot Erosion Test (i.e. HET and SET) (Wan and Fell 2004), and Modified Hole Erosion Test (Luthi et al. 2012). The mechanisms of erosion are similar in HET, SET, and JET. In HET and SET, a hole is drilled in the sample and a water flow is passed through the sample causing further erosion while in JET water jet is applied to the surface of a submerged sample under a constant head. Although, the erodibility trends of various materials are similar in JET and HET, the factors contributing to erosion, e.g. shear stress and soil particle detachment coefficient, are different (Marot et al. 2011, Wahl 2010). JET has a wider range of applications and can be used for a variety of soil materials (Hanson and Hunt. 2007) while HET is more suitable for piping erosion (Wan and Fell 2004). It is worth noting that use of merely JET may underestimate the erosion rates in the field for sandy and clayey soils that are not submerged (Allen et al. 2010). Although, these laboratory and field tests are useful and cost-effective methods to identify the erosion rates, their use in prediction of the erosion rates of overtopped levee-floodwall tests is limited. The reason is that the hydraulic characteristics and erosion mechanism of overtopped floodwalls is not represented with any single test mentioned (Shafii et al. 2016). Therefore, currently there is no established procedure to integrate these tests in designs of levees for erosion resistant purposes.

Many flume type tests were also conducted to identify the erosion rates in levees or levee-floodwall system (Pan et al. 2015, Do et al. 2016, Yu et al. 2013, Hughes and Nadal 2009, Johnson et al. 2013). All the aforementioned studies, except Johnson et al. (2013), were focused on levee overtopping. They ranged from scaled to full-scaled models. In majority of these tests, the soil was coarse-grained material and mainly sand. Johnson et al. (2013) studied the scour characteristics of levees on a scaled model levee-floodwall system with a 1:3 slope, a 57 cm toe length, and various floodwall heights. The soils used in that study had a sand-clay ratio of 60-40% with 76% to 83% compaction levels. It was concluded that the scour depth in those tests would change at an exponential rate and ultimate scour depth can be predicted. While Johnson et al. (2013) provide a more representative erosion mechanism of levee-floodwall systems than other flume type tests and the aforementioned lab tests, there were some limitations although wave action was also practiced in that research: 1) the test results are for a very specific soil profile, 2) the levees with more fine grained material were not tested, 3) a linkage between index lab test results and scour depths and erosion rates was not established. Therefore, there is yet a need for a methodology to determine erosion rates and ultimate scour depth behind the floodwalls which considers soil and hydraulic properties.

1.3 Erosion in Cohesive Soils vs. Cohesionless Materials

In coarse-grained materials (i.e. cohesionless materials), the erosion occurs by relocation of soil particles driven by the induced shear stress. A lot of research has been conducted on erosion of levees and other embankments due to overtopping on both cohesive soils and cohesionless soils (Wei et al. 2016). Experimenting on cohesionless soils is difficult, because a larger lab scaled test would be needed to provide representative conditions of the actual embankments. The minimum material size and the minimum dimensions of earthen embankments required to perform scouring tests on non-cohesive soils have been studied (Schmocker and Hager 2009). Moreover, three correlations were proposed by Schmocker and Hager (2012) to correlate the relationship the breach development and the embankment dimensions and sediments sizes. In another study, it was found that under constant water level overtopping events, the shape of the developed breach is curved (Coleman et al. 2002). The scouring process in cohesive soils is more complicated than non-cohesive soils due to the mechanism of scour (Wei et al. 2016). Reaching the ultimate depth of scour takes a very short time for non-cohesive materials while it might take years for an embankment made with cohesive soils to reach the ultimate depth of scour (HEC-18 Manual 2012). For embankments without floodwalls like dams or dikes constructed with cohesive materials, the scouring procedure starts with headcut erosion (Zhu 2006). In the previous literature, the process of breach through headcut erosion have been studied with scaled laboratory tests (Zhang et al. 2009; Hanson 1999; Zhu 2011). Several estimating models for headcut erosion due to overtopping have also been developed (Hanson et al. 2001; Stein and LaTray 2002; Zhao 2016). Yet, not as many studies have been conducted on floodwall overtopping.

1.4 Objectives

This study aims to provide: 1) a comparison of erosion rate measured from lab tests such as EFA and JET methods versus levee-floodwall systems for fine grained soils with a focus on compaction levels, plasticity indices and saturation levels, 2) a methodology that predicts erosion rates for overtopped lab-scaled levee-floodwall systems given the geotechnical and hydraulic properties, 3) a methodology that predicts erosion rates for overtopped levee-floodwall systems when the EFA and JET tests results are available. This study will provide a better understanding of using EFA and JET in levee erosion studies and is useful for new levee-floodwall design the determination of erosion rates for existing levee-floodwall systems' resistance before and during storm events.

CHAPTER 2

METHODOLOGY

A series of lab-scaled levee-floodwall overtopping, EFA, and JET tests were performed on various soil materials under various flow-rates and floodwall heights. The utilized silty and clayey materials in these tests had Plasticity Indices (PI) of 0% to 9%; Compaction Levels (CL) of 70% to 95%; and 4 ranges of Saturation Ratio ranging from low to high.

2.1 Levee-Floodwall Tests

Levee-floodwall models were constructed in the laboratory with the scales of 1:20 and 1:2 of a full-scaled levee-floodwall. A 2.1 m (7 ft) high floodwall which is a typical floodwall height in levees in New Orleans was assumed as the prototype floodwall. For the 1:20 scaled model, a 49- cm high wooden plate was embedded 35 cm into the levee crest representing a floodwall with 14 cm exposed height. Figure 1 shows a sketch of the 1:20 scaled model as an example. In this study, the overtopping nappe was assumed and designed to be flowing on the floodwall; however, there are cases when water freefall over the floodwall occurs as well.

The 1:2 scaled floodwall was represented by embedding a 142 cm high wooden plate into the levee crest leaving 107 cm of the wall exposed. It is worth mentioning that the levee dimensions remained the same as 1:20 scaled model and the scale represents the height of the floodwall. As a result of different floodwall heights, under the same overtopping flow rate, the velocity at impingement to the levee crest is expected to vary. The other dimensions of the constructed levees remained identical for both scaled models. Plexiglas and transparent sheets were used on the sides of the levee in order to monitor the cross section of the overtopped levee-floodwall during the test.

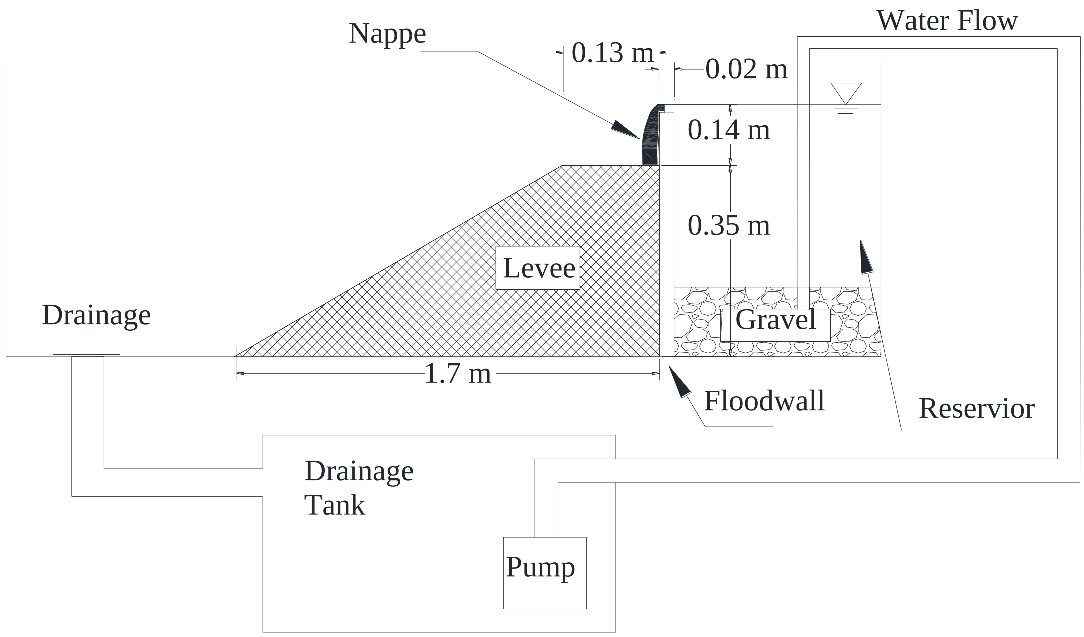

Figure 1. Sketch of the 1:20 scaled levee-floodwall model

The levees were constructed at Compaction Levels (CL) of 70%, 80%, and 90% of the maximum dry unit weight in 5 lifts to cover a wide variety of compaction levels expected in the field. The compaction procedure and the required number of blows with hand tamper to achieve the targeted maximum dry density was identified through several trial and error processes before running the tests. After each layer was compacted, the compaction level was verified by taking 3 samples from right, middle, and left side of the levee. Compaction levels higher than 90% were not achieved in the trial levees due to the large size of the model; however, in the following chapters, a compaction level of 95% is also utilized for JET and EFA. It is worth noting that these trial levees were not used for erosion tests. As noted earlier, the plasticity indices of soils were 0%, 6% and 9% in these tests. More details of the material are provided later in the Chapter 3.

Prior to overtopping in flood events, rainfall saturates the upper layers of the levee soils. Therefore, it was planned to construct levees with various saturation levels. To do so, water was sprayed on the prepared levee surface and was allowed to infiltrate through. The saturation ratio of samples taken from the levee surface was determined. Through a trial and error process, the required amount of water to be sprayed to reach the desired saturation ratio was identified. Four different saturation groups were targeted in this study. The Saturation Ratio (SR) of 0-40%, 40-60%, 60-80%, and 80-100% are referred to as SR 1, SR 2, SR 3, and SR 4, respectively, herein.

After the levee was constructed with the desired CL, PI, and SR, the reservoir behind the floodwall was filled with water. To minimize the water turbulence, the pipe used to fill the reservoir was buried under gravel. After the reservoir was filled, the water overtopped the floodwall with controlled flow-rates of 3 m^3/hr and 4 m^3/hr for the 1:20 scaled model and 2 m^3/hr and 3 m^3/hr for the 1:2 scaled models. As most tests were conducted under the flow-rate of 3 m^3/hr, only these results are discussed thoroughly in Chapter 4. The water overtopping velocity and impingement velocity at the levee crest were determined knowing the applied flow rate, the width of the crest (i.e. 22.9 cm), and the thickness of the generated nappe at the floodwall top edge and just before impingement, respectively (see Figure 1). The nappe thicknesses were measured with a caliper. The nappe thicknesses were also verified by checking the side-view video captured during the overtopping. The water impingement velocity varied from 0.6 m/s to 1.7 m/s depending on the test. A total of 45 levee-floodwall tests were conducted. The soil and hydraulic properties of these tests are shown in are shown in Table 1.

Table 1. List of Levee-Floodwall tests

Levee-Floodwall Tests					
Test No.	**PI (%)**	**CL (%)**	**SR (%)**	**Q (m^3/hr)**	**Scale**
1	0	70	44	3	1:20
2	0	70	48	3	1:20
3	0	70	70	3	1:20
4	0	70	35	3	1:20
5	0	70	24	3	1:2
6	0	70	54	3	1:20
7	0	80	44	3	1:20
8	0	80	75	3	1:20
9	0	80	20	3	1:20
10	0	80	23	3	1:20
11	0	80	26	3	1:2
12	0	80	61	3	1:20
13	0	90	44	3	1:20
14	0	90	80	3	1:20
15	0	90	41	2	1:2
16	0	90	48	3	1:2
17	0	90	70	3	1:20
18	0	90	48	3	1:20
19	0	90	46	3	1:2
20	0	90	46	3	1:20
21	6	70	68	3	1:20
22	6	70	19	3	1:20
23	6	70	30	3	1:2
24	6	70	41	3	1:20
25	6	80	91	5	1:20
26	6	80	30	3	1:20
27	6	80	30	3	1:20
28	6	80	38	4	1:20
29	6	80	72	4	1:20
30	6	80	42	3	1:2
31	6	80	44	3	1:20
32	6	90	47	3	1:20
33	6	90	43	2	1:2
34	6	90	39	3	1:2
35	6	90	28	3	1:2
36	6	90	53	3	1:20
37	9	70	49	3	1:20
38	9	70	40	3	1:2
39	9	70	51	3	1:20
40	9	80	47	3	1:2
41	9	80	61	3	1:20
42	9	90	48	2	1:2
43	9	90	48	3	1:2
44	9	90	53	3	1:2
45	9	90	55	3	1:20

Based on the strength of the material, each levee showed some resistance before the initiation of the scouring process. Once the scouring initiated, the scour depth behind the floodwall was measured at 15 second intervals during the tests. A ruler was placed on the floodwall and the measurements were done later from the test videos. In many of the conducted levee-floodwall tests, a water pool was formed in the developed scour hole. Therefore, the induced shear stress by the water was dissipated within the pool before contacting the soil surface at the bottom of the scour hole. As the pool depth increased, the erosion rate of the levee decreased until a constant or minimal erosion rate was achieved. The time to reach the constant erosion rate is called equilibrium time in this study. After reaching the constant erosion rate, the tests were continued until the levee material was washed away. The average erosion rates presented in this thesis were calculated by dividing the scour depth at the equilibrium condition by the elapsed time from initiation of scouring to the equilibrium time.

2.2 Erosion Function Apparatus

Amongst many index tests that are used to evaluate the influence of soil and hydraulic properties on soil erosion, EFA is one of the most commonly utilized erosion tests where the soil sample surface is eroded by a horizontal controlled flow. The erosion rate is measured using various flow rates in the flume (Briaud et al. 2001).

Figure 2 shows the sketch of an EFA test. EFA test is intended to be conducted on undisturbed soil samples retrieved by Shelby Tubes. However, for the purposes of this study, the samples were reconstructed inside Shelby Tubes to match the levee-floodwall tests' material specifications. The targeted compaction levels for these samples were 70%, 85%, and 95% of the maximum dry density. It was determined that the constructed samples require 9, 18, and

36 hours soaking time to reach 40-60% (i.e., SR 2), 60-80% (i.e., SR 3), and 80-100% (i.e., SR 4) saturation ratios, respectively.

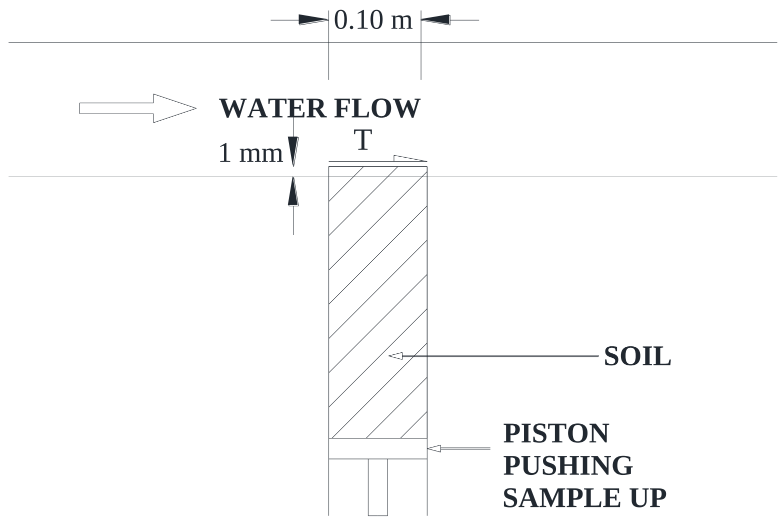

Figure 2. Schematic of EFA test (modified after Briaud et al. 2001)

The EFA samples characteristics are shown in Table 2. The prepared samples were eroded under the flow velocities of 1 m/s, 2.5 m/s, and 5 m/s to cover a wide variety of common flow velocities during levee-flood overtopping. A semi-linear graph of erosion rate versus flow velocity was then plotted in general accordance with Briaud et al. (2001).

Table 2. List of EFA Tests

EFA Tests			
Test No.	**PI (%)**	**CL (%)**	**SR (%)**
1	0	70	67
2	0	85	59
3	0	95	96
4	6	70	65
5	6	85	92
6	6	85	67
7	6	95	56
8	9	70	94
9	9	85	86
10	9	95	80

2.3 Jet Erosion Test

A JET apparatus was constructed in the laboratory following the specifications of ASTM D5852 and Hanson and Cook (2004). For each jet erosion test, a soil sample with a diameter of 44 cm was constructed to match the soil specifications used in the levee-floodwall and the EFA tests and was submerged in the JET tank. Then, the sample was eroded under a water jet through a submerged nozzle with a diameter of 1.3 cm located 22 cm above the submerged sample. Figure 3 shows the details of the JET apparatus. The soil profile and the scour depth at the midpoint of the samples were measured at 600, 1800, 3600, and 7200 seconds during the duration of each test. The water velocity, shear stress, critical shear stress, and consequently erosion rates were determined using Hanson et al. (2002) and Hanson and Cook (2004) methodologies. The JET samples specifications are shown in Table 3.

Table 3. List of JET tests

JET Tests		
Test No.	**PI (%)**	**CL (%)**
1	0	70
2	0	85
3	0	95
4	6	70
5	6	85
6	6	85
7	6	95
8	9	70
9	9	85
10	9	95

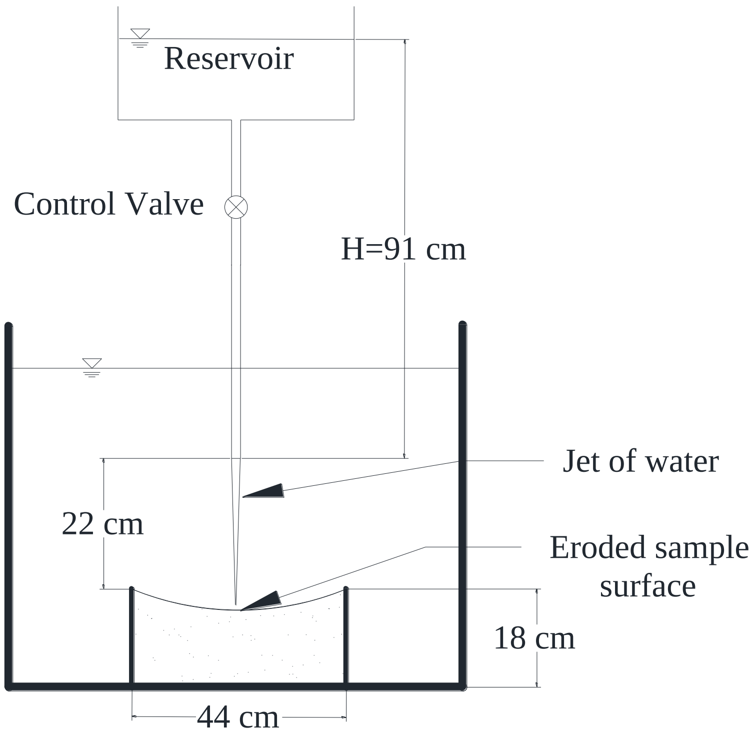

Figure 3. Schematic of Jet Erosion Test

Critical shear stress and effective shear stress are the two important parameters required to calculate the erosion rate using JET per ASTM D 5852. Effective shear stress is the induced shear stress at the soil surface and critical shear stress is defined as the minimum shear stress applied to the soil to initiate scouring. There are many proposed correlations for calculating these parameters (Hanson and Cook 2004; Rajaratnam and Beltaos 1977; Phares et al 2000; Carrillo 2015; and Ghaneeizad et al. 2015). In this paper, the method proposed by Hanson and Cook (2004) was utilized due to its accuracy compared to the other proposed methods.

CHAPTER 3

MATERIAL

For the conducted tests in this study, two types of fine-grain soils typically found in the Mississippi River banks were used. Particle Size Analysis and Atterberg Limit tests were performed on the retrieved soils in general accordance with ASTM D6913, and ASTM D4318, respectively. The soils were classified as sandy SILT (ML) and sandy LEAN CLAY (CL) based on Unified Soil Classification System with Plasticity Index of 0% and 12%, respectively. The soils used for the conducted tests consisted of ML soil and two mixtures of ML and CL soils: 1:1 ratio of ML and CL, and 1:2 ratio of ML and CL. Atterberg Limits test was conducted on the mixtures and it was found that 1ML:1CL and 1ML:2CL, which are both classified as ML-CL based on USCS (ASTM D2487) soils, had 6% and 9% Plasticity Indices (PI), respectively. The mixtures are distinguished by their plasticity indices throughout the paper. Sieve Analysis, Hydrometer, and Standard Proctor Compaction Tests were conducted on the mixtures in general accordance with ASTM D 6913, ASTM D 7928, and ASTMD 698, respectively. Figure 4 and Figure 5 show the results of particle size analysis and compaction curves of the aforementioned soil samples, respectively.

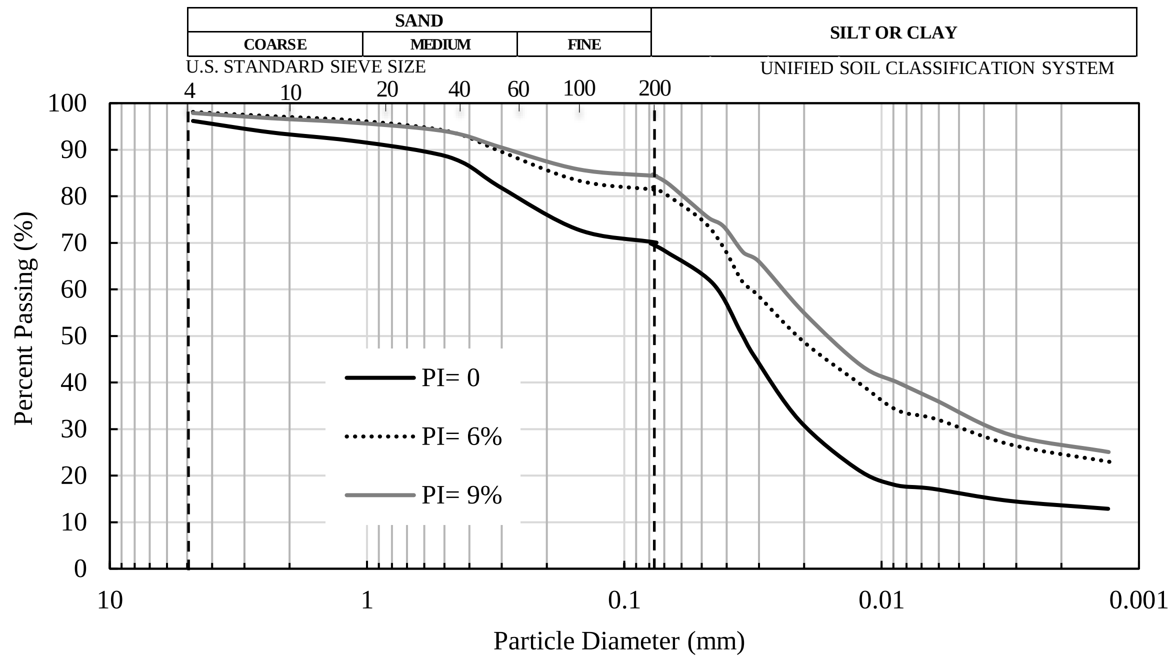

Figure 4. Particle Size Analysis for soil materials with PI of 0, 6%, and 9%

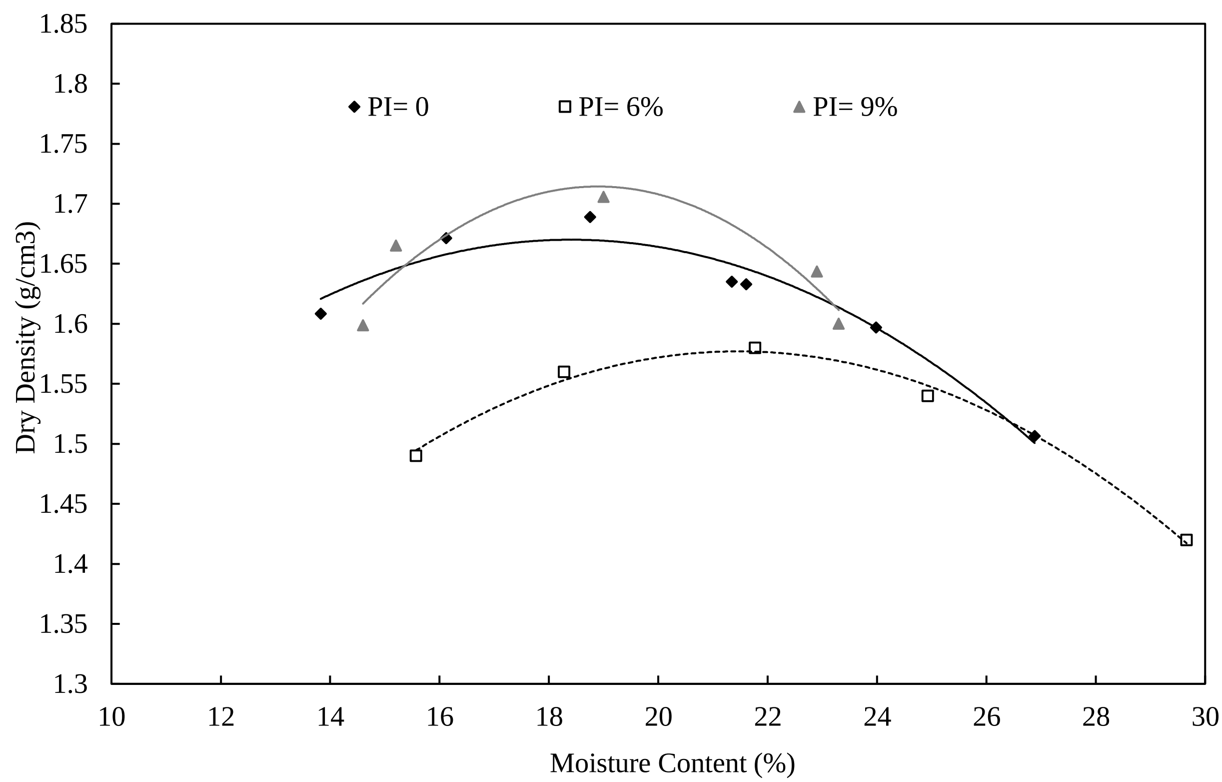

Figure 5. Standard Proctor Compaction curve for samples with PI of 0, 6%, and 9%

CHAPTER 4

RESULTS AND DISCUSSION

4.1 Levee-Floodwall Tests

As the pool depth increased due to the development of a scour hole, the rate of erosion decreased throughout the test. The decreasing rate of erosion is shown in Figure 6 and 7 for 1:20 and 1:2 scaled levee-floodwalls, respectively. The flow-rate for these tests was 3 m^3/hr. It is observed that regardless of the soil plasticity index and compaction level, the erosion rate continued to decrease until it reached equilibrium condition. It can be seen in Figure 6 and 7 that the measured erosion rate was zero for almost all the tests for the first few seconds after the overtopping was initiated. As an example, the sample with a PI of 9% and CL of 90% in 1:20 scaled test shown with hollow circle symbols in Figure 6 resisted scouring for 32 seconds followed by initial erosion rate of 600 mm/hr. By generation of a deeper pool of water at the scour hole, the decreasing trend of erosion rate leveled off at an approximately constant erosion rate of 350 mm/hr at an approximate elapsed time of 336 seconds after scour initiation. As shown in Figure 6 and 7, the test duration for samples with higher PI and CL was higher which is due to their resistance against the overtopping. The samples with lower PI and CL were washed away after a shorter period of time.

Symbol	■	■ (tan)	□	◆	◆ (tan)	◇	●	● (tan)	○
PI (%)	0	0	0	6	6	6	9	9	9
CL (%)	70	80	90	70	80	90	70	80	90
Scale	1:20								

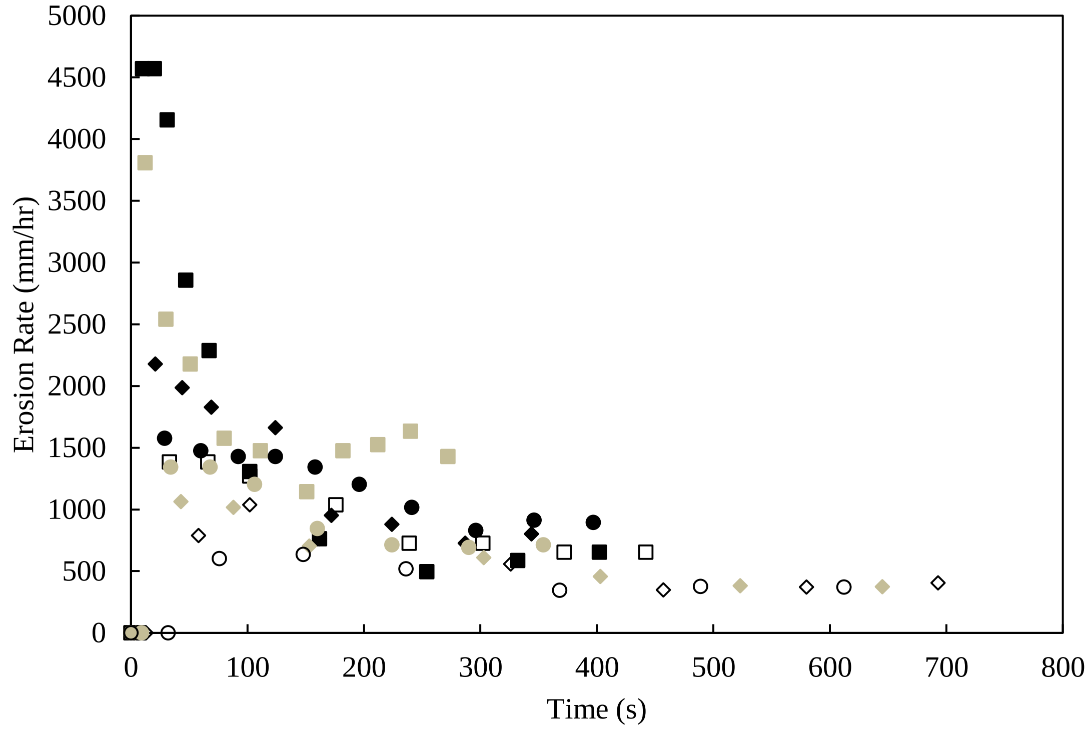

Figure 6. 1:20 scaled levee-floodwall erosion rates subject to 0.2 m/s flow velocity at the top of the wall results throughout testing period

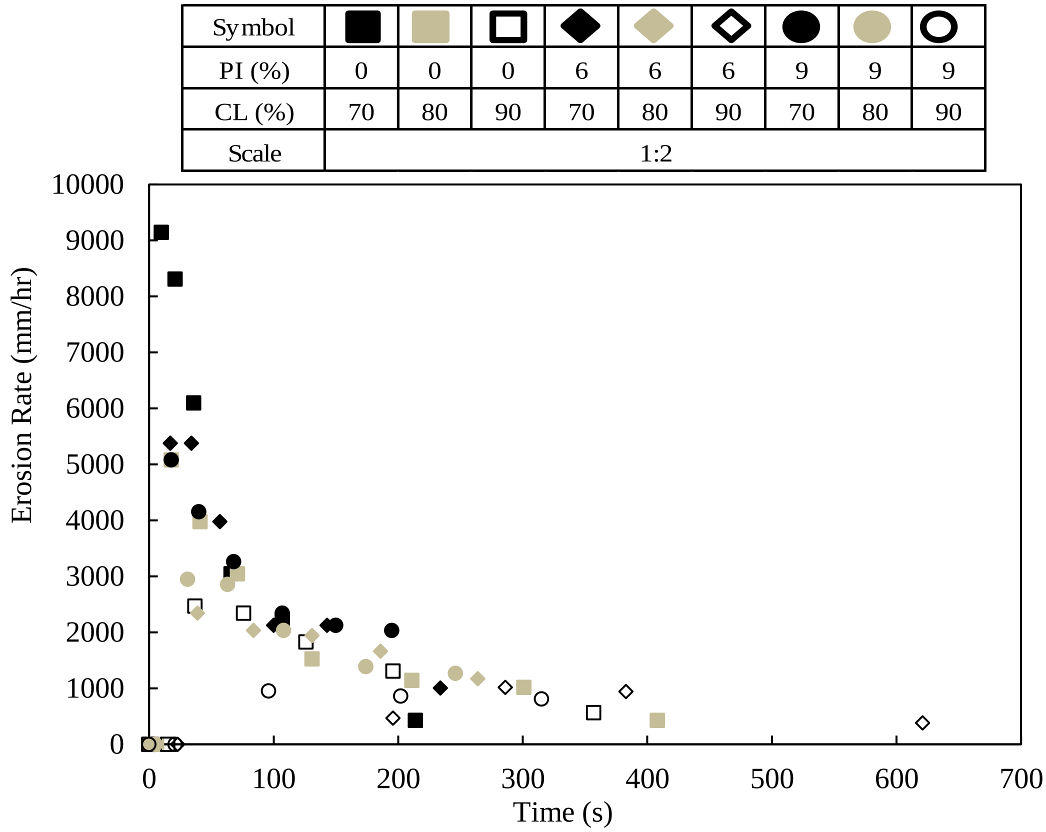

Figure 7. 1:2 scaled levee-floodwall erosion rates results subject to 0.2 m/s flow velocity at the top of the wall throughout testing period

According to Figure 6, the erosion rates for materials with lower PI and CL decrease more rapidly than the materials with higher PI and CL in the first 100 seconds of scour initiation. The reason is the formation of the pool behind the wall in a shorter time frame for lower PI and CL materials that absorbs the water jet energy. For example, the erosion rate reduction for materials with PI of 0% with CLs of 70% and 80% was 73% and 61%, respectively, within the first 100 seconds for 1:20 scaled model tests. However, the erosion rate for the materials with PI of 0 and CL of 90% and the material with PI of 9% and CL of 80% decreased 11% and 9% within the first 100 seconds, respectively. It is observed that the erosion rates are reduced nonlinearly for the weaker soil samples and linearly for the stronger soil samples. Similar observation was made for 1:2 scaled tests shown in Figure 7.

The equilibrium time for 1:2 and 1:20 scaled tests ranges from 100 seconds to 200 seconds and 150 seconds to 300 seconds after the initiation of scouring, respectively. It is expected for a full sized levee-floodwall system, the erosion reaches to equilibrium condition within a few minutes after the initiation of scouring if the overtopping flow remains constant. Regardless of the scale of the levee-floodwall tests, for the materials with PIs of 0%, 6%, and 9%, the ratio of the equilibrium erosion rate to the initial erosion rate ranged from 10% to 30%, 25% to 35%, and 40% to 55%, respectively. This indicates that the major scour occurs in the early stages of the erosion process and prior to equilibrium time.

4.1.1 Plasticity index (i.e. PI) effect

Figure 8 shows the average erosion rate results of the conducted levee-floodwall experiments versus plasticity index. According to this figure, for the 1:20 scaled tests, as the plasticity index for the material increased from 0 to 6%, the erosion rate decreased between 28% and 41% and as the plasticity index increased from 6% to 9% an erosion rate decrease ranging from 13% to 21% was observed. The reductions in the measured erosion rates ranged from 15% to 38% and 23% to 26% for 1:2 scaled models when plasticity index increased from 0 to 6% and from 6% to 9%, respectively. In the 1:2 scaled model, the sample was subject to a larger induced shear stress caused by higher water impingement velocity as the height of the floodwall was larger. This indicates that under higher shear stresses, the increase in PI is less effective in erosion rate mitigation than lower shear stresses. The results of this figure also show that the effect of change in plasticity index on erosion rate is more obvious on samples with lower compaction levels. It is worth noting that by changing the scale from 1:20 to 1:2, the erosion rates increased by a factor of 1.7 to 2, 1.4 to 2.8, and 1.8 to 2.3 for the PIs of 0%, 6%, and 9%, respectively.

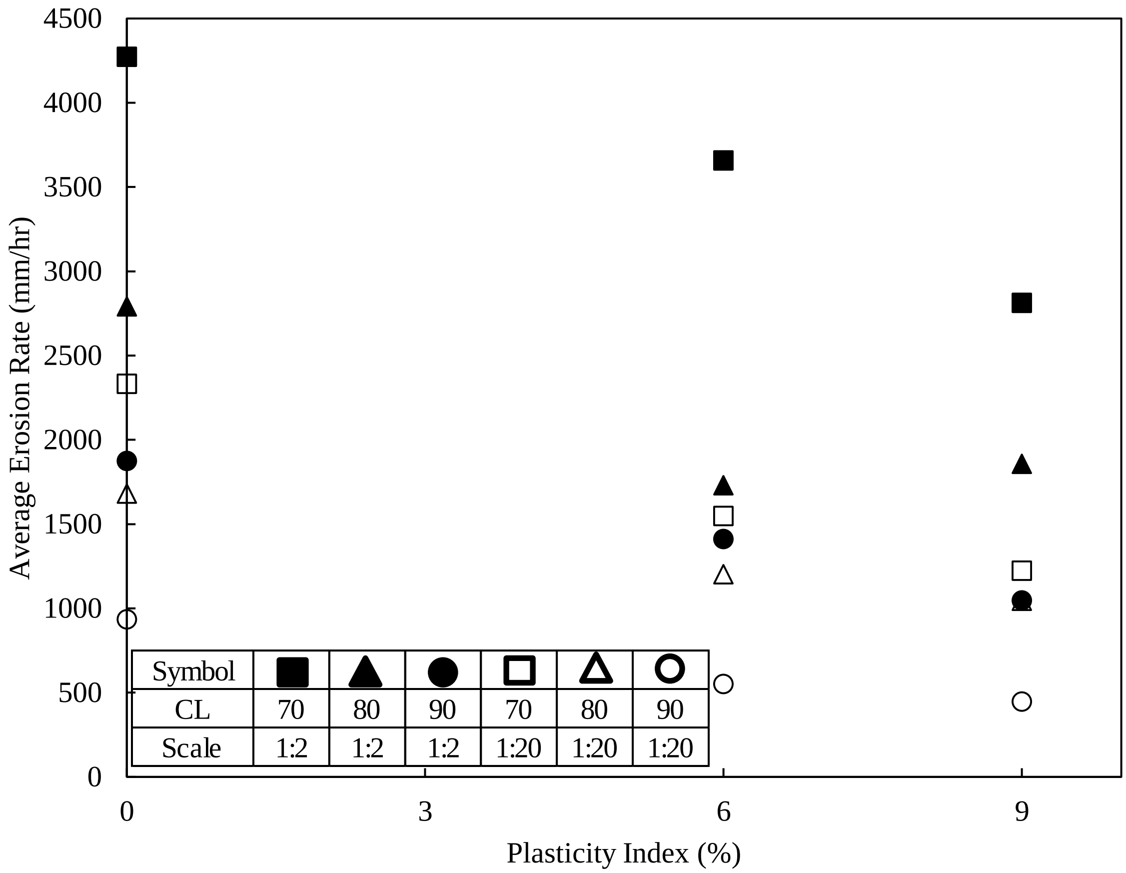

Figure 8. Levee-floodwall average erosion rates variation with plasticity index

4.1.2 Compaction level (i.e. CL) effect

Figure 9 shows the average erosion rate results of the conducted levee-floodwall experiments versus compaction level. Due to the higher number of available 1:20 scaled conducted tests, each point shown on Figure 9 is an average of several representative tests with the same PI and CL; however, for the 1:2 scale each point represents the results of a single test. It can be concluded from Figure 9 that the rate of decrease in erosion rate as a result of increasing compaction level for non-plastic material is similar for both 1:20 and 1:2 scales. In the 1:20 scaled tests with non-plastic material, as the compaction level for the material increased from 70% to 80% and from 80% to 90%, the erosion rate decreased by 28% and 44%, respectively. The reduction in erosion rates were 35% and 33% for the same material tested in the 1:2 scaled model when compaction level increased from 70% to 80% and from 80% to 90%, respectively. For higher plasticity material, the change in compaction level would result in a nonlinear reduction in erosion rate for the 1:20 scale and a linear reduction in erosion rate for the 1:2 scale. For these materials the reduction in erosion rates can be as low as 14% and as high as 57% for the conducted tests when compaction levels change from 70% to 80 % and 80% to 90%, respectively.

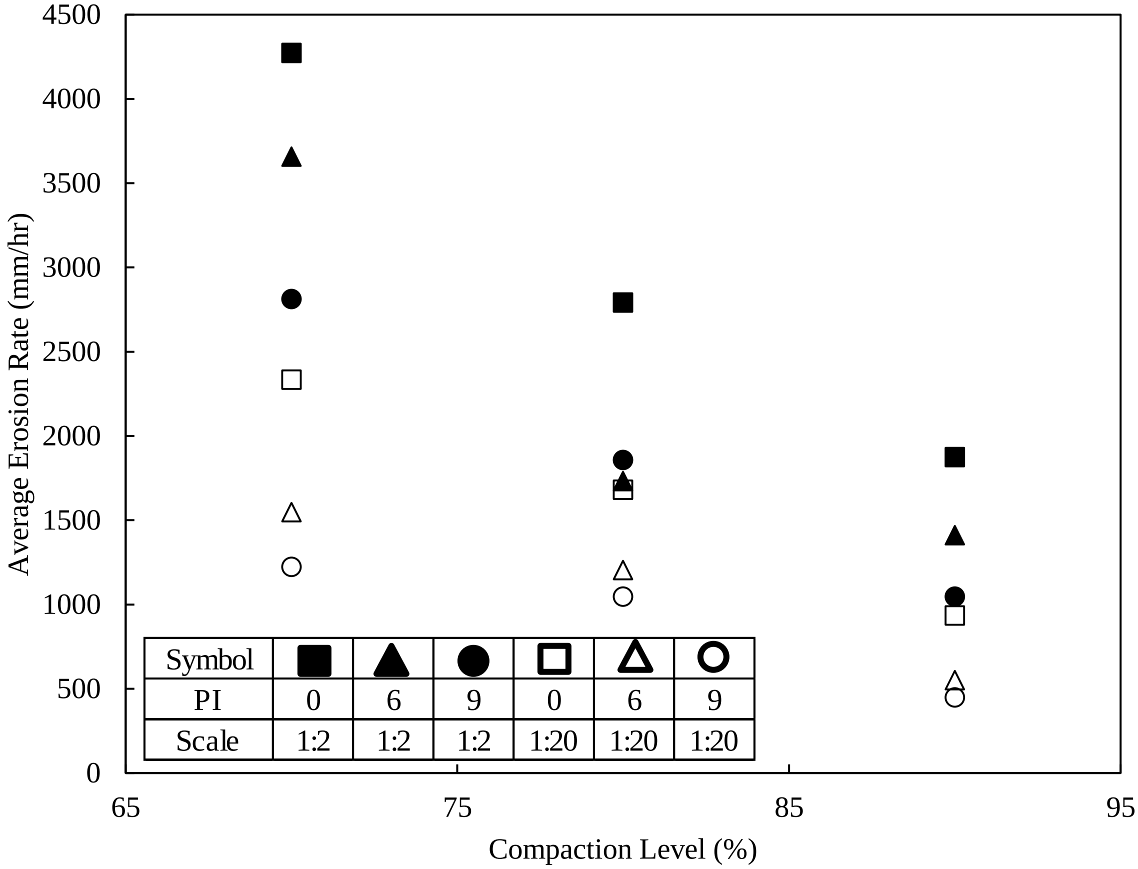

Figure 9. Levee-floodwall average erosion rates variation with compaction level

The erosion rate of samples with 90% compaction level are approximately 0.4 of the erosion rates of samples with 70% compaction while the erosion rate of samples with PI of 9% are 0.6 of samples with PI of 0. It is concluded that in the conducted levee-floodwall tests, increasing the compaction level is slightly more effective on erosion rate reduction than increasing the plasticity index.

4.2 Erosion Function Apparatus (i.e. EFA) Tests

To have consistent results with the conducted levee-floodwall tests, EFA samples were prepared with the same specifications of the tested levee materials (see Table 1b). The samples were tested under the water flow velocities of 1, 2.5, and 5 m/s and the results are shown in Figure 10. Plasticity index, compaction level, and saturation ratio as the dominant soil properties in erosion characteristics of materials affect the erosion rates of the EFA samples similar to trends observed in levee-floodwall tests (Karimpour et al. 2015; Osouli et al. 2017). However, the magnitude of the erosion rate was up to 2 times less in EFA tests compared to 1:2 levee-floodwall tests.

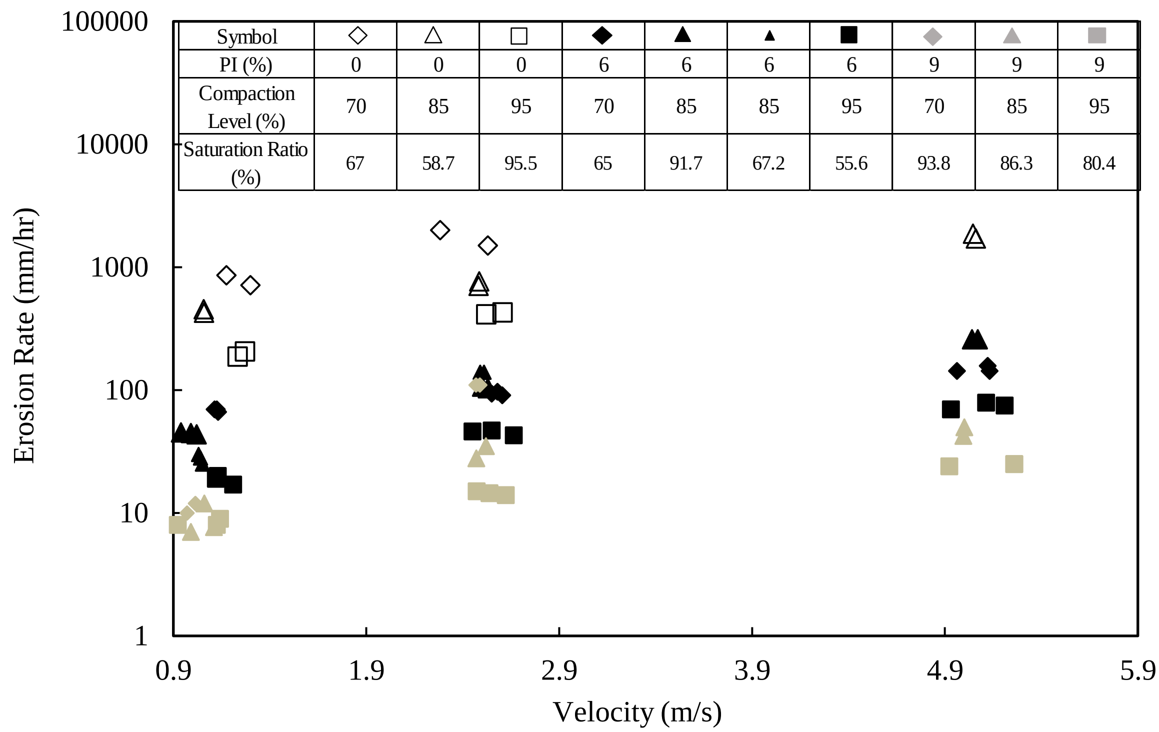

Figure 10. Measured erosion rate versus velocity for conducted EFA tests

It can be concluded that the erosion rate of samples with 95% compaction level are approximately 0.4 to 0.5 of the erosion rates of the samples with 70% compaction while the erosion rate of the samples with PI of 9% are 0.10 to 0.15 of that of samples with PI of 0. This shows that the plasticity index is a more dominant factor in erosion mitigation than the compaction level while in the levee-floodwall tests an opposite conclusion was made.

By increasing the flow velocity from 1 m/s to 2.5 m/s, the erosion rate increased by a range of 66% to 225% for various soil configurations while by increasing flow velocity from 2.5 m/s to 5 m/s, the erosion rate increased by a range of 20% to 124% for the conducted tests. Since the flow velocities for the levee-floodwall tests at the impingement were less than 2 m/s, the EFA erosion rate results for the flow velocity of 1 m/s are used in the following sections to develop levee erosion prediction models. It is noteworthy that the water impingement velocity of 1 to 3 m/s was also commonly estimated for overtopped floodwalls during Hurricane Katrina (IPET 2006).

4.3 Jet Erosion Tests (i.e. JET)

The samples with specific characteristics shown in Table 1c were prepared for JET samples. They were constructed with PIs of 0%, 6%, and 9% and CLs of 70%, 85%, and 95%. Unlike EFA, the impingement velocity of water in JET could not be measured directly since the sample was submerged; therefore, it needed to be calculated in accordance with Hanson et al. (2002).

Figure 11 shows the results of the conducted JET tests. For each test, there are 4 points in this figure representing the measured erosion rate at 600, 1800, 3600, and 7200 seconds. Point 1 has a 6 to 9 times higher erosion rate than Point 4. Since the measurement of erosion rate of Point 1 requires less time, the erosion rates of Point 1 was used in the later sections of this paper for the purpose of developing the prediction models.

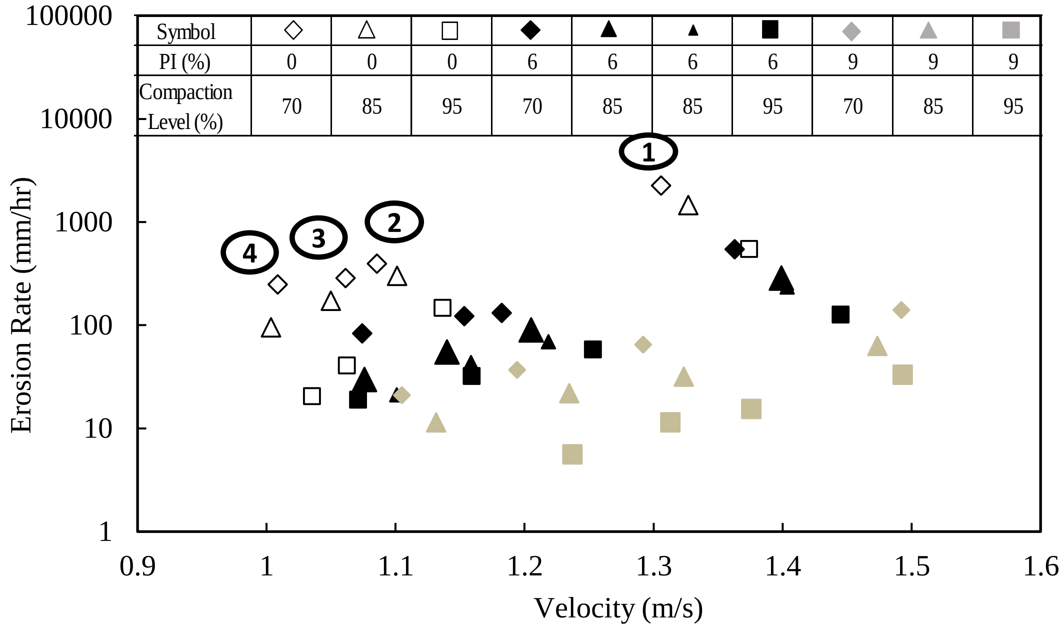

Figure 11. Erosion rate versus velocity for JET test results

The comparison of the erosion rate for Point 1 of the JET tests shows that erosion rates of samples with 95% compaction level are approximately 0.25 of the erosion rates of samples with 70% compaction while the erosion rates of samples with PI of 9% are 0.06 of samples with PI of 0. Therefore, similar to EFA results discussed in the previous section, increasing PI is more effective than CL in JET. The Same conclusion was made by Hanson and Hunt (2007). However, this finding opposes the conclusions made in the levee-floodwall test results.

CHAPTER 5

PREDICTION MODELS

5.1 Levee Erosion Prediction Model Based on Soil Properties (i.e., Model 1)

Based on the obtained levee average erosion rates subject to various PI, SR, CL, flow overtopping velocity at the top of the floodwall, and scale, a prediction model was proposed to produce an estimate for the average erosion rates of a given levee-floodwall without the need to run any direct laboratory or field testing. Model 1 is based off a base erosion rate of 1,933 mm/hr. The base erosion rate represents the erosion rate of a levee with PI of 0, CL of 70%, SR Group of 1, flow overtopping velocity of 0.2 m/s, and floodwall scale of 1:20. The base erosion is corrected with coefficients associated with PI, SR, CL, flow overtopping velocity at the top of the floodwall, and scale to match the erosion rate for a specific soil configuration as shown by Equation 1.

$$\dot{\varepsilon}\left(\frac{mm}{hr}\right) = 1933\,.\,\delta_{PI}.\,\delta_{SR}.\,\delta_{CL}.\,\delta_{FV}.\,\delta_{Scale} \quad (1)$$

Where,

$\dot{\varepsilon}$: Levee Average Erosion Rate

δ_{PI}: Plasticity Coefficient,

δ_{SR}: Saturation Ratio Coefficient

δ_{CL}: Compaction Level Coefficient

δ_{FV} : Coefficient for Overtopping Flow Velocity at the Top of the Floodwall

δ_{Scale} : Scale Coefficient

The values for the above coefficients were optimized using MS Excel solver function to minimize the error between the measured and the predicted erosion rates. The coefficients are shown in Table 4.

Table 4. Coefficients of prediction Model 1

PI (%)	δ_{PI}	**SR Group**	δ_{SR}	**CL (%)**	δ_{CL}	**Overtopping Velocity (m/s)**	δ_{FV}	**Scale**	δ_{Scale}
0	1	1	1	70%	1	0.2	1	1:20	1
6	0.62	2	1.19	80%	0.51	0.3	2.74	1:2	3.4
9	0.51	3	1.42	90%	0.32				
		4	2.39						

Model 1 was generated using materials with PIs of 0 to 9% and the measured versus predicted values are shown in Figure 12 with solid symbols. The measured and Model 1 predicted erosion rates for the PIs ranging from 0% to 9% show a reasonable agreement. To examine the validity of the model in levees with high PIs, six additional levee-floodwall tests were tested with PIs of 30% and 40% and CLs of 70%, 80%, and 90% to mimic some of the levees with high PIs in New Orleans (IPET 2006). The estimated erosion rates for these tests by Model 1 and the observed filed erosion rates are shown in Figure 12 with hollow symbols. The results were within reasonable agreement for tests with PI=40% and CL=90% and CL=80%; however, the measured erosion rate for the PI=30% with CL=70%, CL=80% and CL=90% samples were significantly higher than the predicted erosion rates.

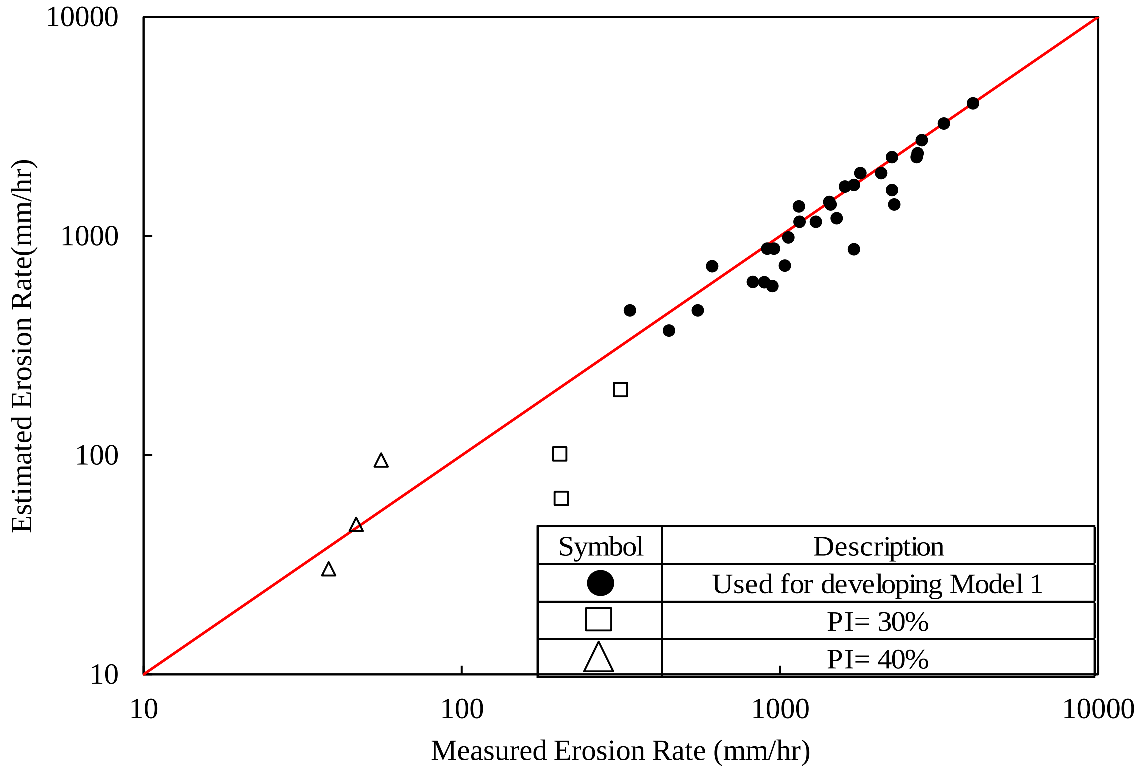

Figure 12. Levee-floodwall erosion rate predictions and measurements represented by Model 1

5.2 Levee Erosion Prediction Model Based on JET and EFA (i.e., Model 2)

The EFA and JET together can represent the complicated erosion mechanism in levee-floodwall systems. In EFA and JET the soil surface is eroded with horizontal and vertical flows, respectively. However, the overtopping nappe in levee-floodwalls has a slight angle from the vertical. Therefore, Model 2, represented by Equation 2, is developed to predict the erosion rates in levee-floodwall tests using the EFA and JET results. As noted earlier, the EFA erosion rates under 1 m/s flow velocity and the JET erosion rates at the first 600 seconds were used for the development of Model 2. The variables of this equation are described in Table 5.

$$\dot{\varepsilon} = SDQF\sqrt{C_1 J^2 + C_2 E^2} \quad (2)$$

Table 5. Variables of prediction Model 2 for Predicting Levee-Floodwall Erosion Rates Using JET and EFA Test Results

Variable	**Description**	**Value**
S	Saturation ratio factor	$\sqrt{\frac{\text{Levee saturation ratio}}{\text{EFA sample saturation ratio}}}$
D	JET diffusion factor	1, 2.3, 7.5 for plasticity indices of 0, 6, and 9 respectively
Q	Flow rate factor	$\left(\frac{\text{Flow rate }(\frac{m^3}{hr})}{3}\right)^3$
F	Scaling factor	$2.5887 \times \text{H} + 0.64$
H	Exposed Floodwall Height (m)	
C_1	JET weight factor	2.6
C_2	EFA weight factor	1
J	JET erosion rate at 600s interval (mm/hr)	Measured from test
E	EFA erosion rate at 1m/s(mm/hr)	Measured from test

Out of the 45 performed levee-floodwall tests, 17 test results were used to derive the prediction model. The other remaining 28 test results were used to verify the developed prediction model. Figure 13 shows the predicted levee erosion rate using Model 2 versus actual measured erosion rates for the 28 performed simulated levee-floodwall tests.

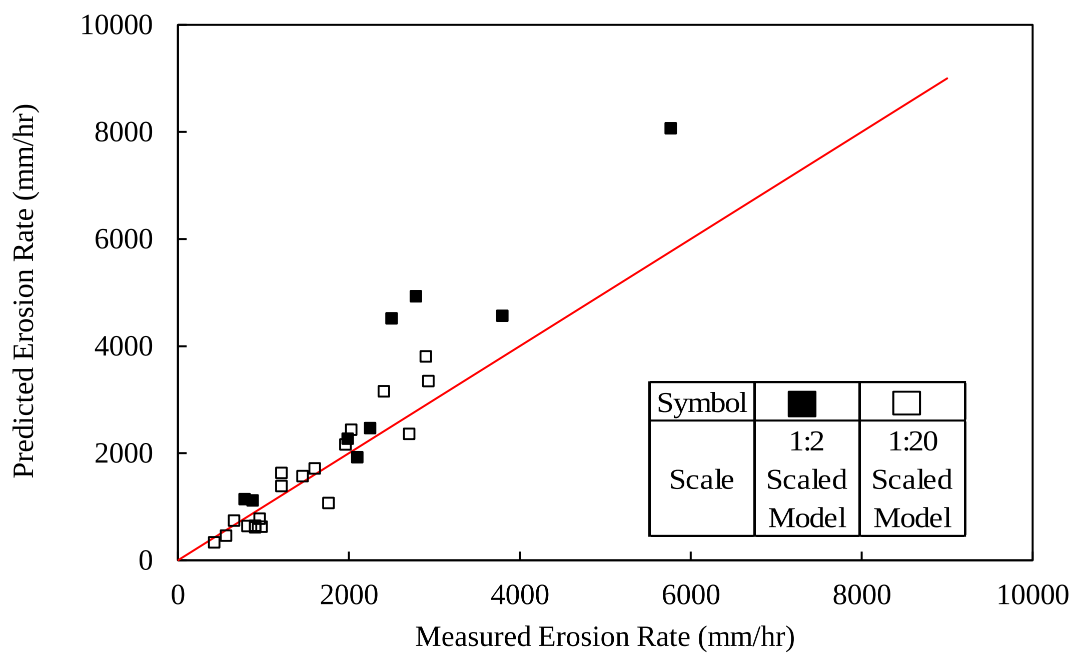

Figure 13. Levee-floodwall erosion rate predictions using JET and EFA test results and Model 2

Out of 28 levee-floodwall tests used for verification, erosion rates for 25 of them were predicted with minimal error with a root mean square deviation of less than 20%. Most of these tests had erosion rates of lower than 4000 mm/hr. Only in 3 remaining tests, the predicted erosion rates were up to 30% higher than the measured values on the conservative side. The mentioned 3 tests with Test Nos. of 5, 11, and 38 (see Table 1 for details) had the lowest compaction level or the lowest plasticity index and were exposed to high floodwall height.

Overall, it can be concluded the proposed correlation can provide a reasonable estimation of erosion rates for the overtopped floodwalls.

The EFA coefficient (C_2) is the weight factor for EFA erosion rate at 1 m/s water velocity in the proposed model. It was shown in the performed tests that the erosion rates in EFA tests are significantly lower than the erosion rates in levee and JET tests. Therefore, Model 2 can be simplified by ignoring the EFA coefficient (i.e., $C_2 = 0$). If EFA is eliminated from Model 2, the saturation ratio factor 'S' (see Table 5) becomes irrelevant, because the JET sample is a submerged saturated sample and saturation ratio would not be applicable. The simplified model is described by Equation 3.

$$\dot{\varepsilon} = DQF\sqrt{C_1 J^2} \quad (3)$$

The erosion rates of the performed levee-floodwall tests were re-predicted with the simplified prediction model. Figure 14 shows the new estimation of levee erosion rates using merely JET results for all 45 levee-floodwall tests.

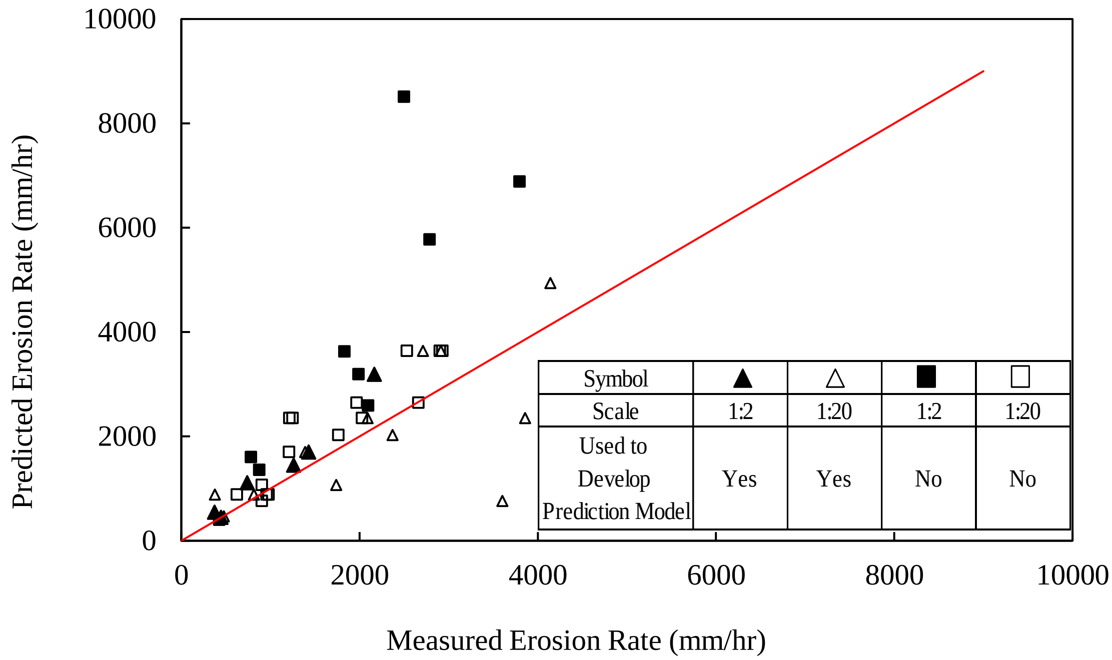

Figure 14. Levee-floodwall erosion rate predictions using simplified Model 2

As expected, more scattered prediction results are observed; however, the simplified version of Model 2 shows less scattering in the lower than 3000 mm/hr erosion rates. Also, the predicted erosion rates are higher than the measured erosion rates in most cases. It is shown that by neglecting the EFA results, the simplified model provides a rough estimate of the erosion rate but with a higher root mean square deviation (i.e., 30%) and on the conservative side. The simplified model has the following advantages for estimations of levee erosion rate: 1) The test can be performed in-situ using field Jet Erosion Test apparatus; 2) It eliminates the complexity of running the expensive test of EFA and taking undisturbed samples; 3) It provides a rough, but reasonable, estimate of erosion rate within only 10 minutes of running a JET test.

CHAPTER 6

CONCLUSIONS AND RECOMMENDATIONS

Predicting the erosion rates of levee-floodwall systems during various storm conditions helps design stable levees and evaluate the existing levees' performances during different storm events. In this study, various levee-floodwall tests have been conducted along with EFA and JET tests.

The erosion characteristics of the samples with various soil properties have been compared and the effectiveness of using standardized tests like EFA and JET as alternative tests to actual levee erosion testing is evaluated. It was concluded that EFA and JET have lower erosion rates compared to levee-floodwall tests and using their results together gives a better understanding of the levee erosion characteristics. Moreover, the behavior of various materials were compared using a levee simulator test, EFA, and JET with regard to their compaction level and plasticity index and their effectiveness on erosion mitigation was evaluated. It was found that compaction and plasticity index are the dominant factors affecting the erosion resistivity of levees; however, because floodwall overtopping often occurs after heavy rains, the levee soil will be saturated and the effect of saturation ratio on scouring process can be as important as compaction and plasticity index.

The levee-floodwall test results show that the erosion rates are reduced nonlinearly for the lower resistant materials and linearly for the higher resistant materials. They also indicate that the major part of scour occurs before equilibrium time. Furthermore, two prediction models have been proposed for overtopped levee erosion rates estimation to help engineers predict scouring behaviors of levees built with various fine grain materials and design the floodwall heights under different storm conditions. The models' predictions were evaluated by comparing the estimated erosion rates with the measured ones. It was concluded that the models provide reasonable estimates for the levee-floodwall average erosion rates. The models can be improved by performing tests with more variety of PIs, flow-rates, and scales.

REFERENCES

Allen, P., Capello, S., & Coffman, D. (2010). Comparison of submerged jet testing to field erosion rates in clay and sand channels, blackland prairie ecosystem, Texas. *2nd Joint federal interagency conference.* Las Vegas.

Amini, F., Li, L., & Xu, Y. (2013). Slope stability analysis of three earthen levee strengthening systems under hurricane overtopping flow conditions. *Geo-Congress*, (pp. 1882-1891). San Diego, CA.

ASTM-D5852. (2007). *Standard test method for erodibility determination of soil in the field or in the laboratory by the jet index method.* Philadelphia: Annual book of ASTM standards.

Baars, S. (2004). Peat dike failure in the Netherlands. *Official Publication of the European Water Association (EWA).*

Briaud, J. L., Chen, H. C., Govindasamy, A. V., & Storesund, R. (2008). Levee erosion by overtopping in New Orleands during the Katrina Hurricane. *Journal of Geotechnical and Geoenvironmental Engineering*, 618-632.

Briaud, J., Ting, F., Chen, H., Cao, Y., Han, W., & Kwak, K. (2001). Erosion function apparatus for scour rate predictions. *Journal of geotechnical and geoenvironmental engineering*, 105-113.

Carrillo, V. (2015). Numerical investigation of the shear stress distribution resulting from a turbulent impinging jet. Pullman, WA: MS Thesis, Washington State University.

Chang, T., Chen, S., & Huang, S. (2011). Shelter effect evaluation of the willow works bank protection method: a case study for Beinn River Reach 2009 Typhoon Morakot event. *Paddy and Water Environment, 11*, 15-33.

Coleman, S. E., Andrews, D. P., & Webby, M. G. (2002). Overtopping breaching of noncohesive homogeneous embankments. *Journal of Hydraulic Engineering, 128*, 829-838.

Do, X. K., Kim, M., Thao Nguyen, H. P., & Jung, K. (2016). Analysis of landslide dam failure caused by overtopping. *12th International Conference on Hydroinformatics* (pp. 990-994). Procedia Engineering.

Ghaneezad, S. M., Atkinson, J. F., & Bannett, S. J. (2015). Effect of flow confinement on the hydrodynamics of circular impinging jets: implications for erosion assessment. *Environmental Fluid Mechanics, 15*(1), 1-25.

Hanson, G. J., & Cook, K. R. (2004). Apparatus, test procedures, and analytical methods to measure soil erodibility in situ. *Applied engineering in agriculture*, 455-462.

Hanson, G. J., Robinson, K. M., & Cook, K. R. (2001). prediction of headcut migration using a deterministic approach. *T. ASAE, 44*, 525-531.

Hanson, G. J., Temple, D. M., & Cook, K. R. (1999). Dam overtopping resistance and breach processes research. *Association of State Dam Safety Officials Annual Conference.* St. Louis: CD-ROM.

Hanson, G., & Hunt, S. (2007). Lessons learned using laboratory JET method to measure soil erodibility of compacted soils. *Applied engineering in agriculture*, 305-312.

Hanson, G., Robinson, K., & Cook, K. (2002). Scour bellow an everfall: Part II. Prediction. *Transactions of the ASAE*, 957-964.

Hughes, S. A., & Nadal, N. C. (2009). Laboratory study of combined wave overtopping and storm surge overflow of a levee. *Coastal Engineering, 56*(3), 244-259.

Johnson, E. B., Testik, F. Y., Ravichandran, N., & Schooler, J. (2013, January 1). Levee scour from overtopping storm waves and scour counter measures. *Ocean Engineering*, 72-82.

Karimpour, M., Heinzl, K., Stendback, E., Galle, K., Zamiran, S., & Osouli, A. (2015). Scour characteristics of saturated levees due to floodwall overtopping. *IFCEE*, (pp. 1298-1307).

Luthi, M., Fannin, R. J., & Millar, R. G. (2012). A modified Hole Erosion Test (HET-P) device. *Geotechnical Testing Journal, 35*(4), 1-5.

Marot, D., Regazzoni, P., & Wahl, T. (2011). Energy-based method for providing soil surface erodibility rankings. *Journal of Geotechnical and Geoenvironmental Engineering, 137*(12), 1290-1293.

Osouli, A., Karimpour, M., & Safarian Bahri, P. (2017). Erosion Characteristics of Silty to Clayey Soils Using EFA and Lab-Scaled Levee-Floodwall Tests. *Geotechnical Testing Journal, 40*(3).

Pan, Y., Li, L., & Amini, F. (2015). Overtopping erosion and failure mechanism of earthen levee strengthened by vegetated HPTRM system. *Ocean Engineering, 96*, 139-148.

Phares, D. J., Smedley, G. T., & Flagan, R. C. (2000). The wall shear stress produced by the normal impingement of a jet on a flat surface. *Journal of Fluid Mechanics, 418*, 351-375.

Rajaratnam, N., & Beltaos, S. (1977). Erosion by Impinging Cicular Turbulent Jets. *Journal of the Hydraulics Divisions- ASCE, 103*(10), 1191-1205.

Schmocker, L., & Hager, W. H. (2009). Modelling dike breaching due to overtopping. *Journal of Hydraulic Res., 47*, 585-597.

Schmocker, L., & Hager, W. H. (2012). Plane dike-breach due to overtopping: effects of sediment, dike height and discharge. *Journal of Hydraulic Res., 50*, 576-586.

Shafii, I., Briaud, J. L., Chen, H. C., & Shidlovskaya, A. (2016). Relationship between soil erodibility and engineering properties. *ICSE 2016.* Oxford: Harris, Whitehouse & Moxon (Eds).

Stein, O. R., & LaTray, D. A. (2002). Experiments and modeling of head cut migration in stratified soils. *Water. Resour. Res., 38*, 1284.

Tirpak, S. M. (2009). United States army corps of engineers, Galveston district operational experiences and response to Hurricane Ike. *Shore and Beach, 77*(2), 60-70.

Villarini, G., Smith, J., Baeck, M., & Krajewski, W. (2011). Examining flood frequency distributions in the Midwest U.S. *American water resources association*, (p. 447).

Wahl, T. L. (2010). A comparison of the hole erosion test and Jet Erosion Test. *Joint federal interagency conference on sedimentation and hydrologic modeling.* Las Vegas.

Wan, C. F., & Fell, R. (2004). Investigation of rate of erosion of soils in embankment dams. *Journal of Geotechnical and Geoenvironmental Engineering, 130*(4), 373-380.

Wei, H., Yu, M., Wang, D., & Li, Y. (2016). Overtopping breaching of river levees constructed with cohesive sediments. *Natural Hazards and Earth System Sciences, 16*(7), 1541-1551.

Xiao, H., Huang, W., & Tao, J. (2009). Numerical modeling of wave overtopping a levee during Hurricane Katrina. *Computers and Fluids, 38*(5), 991-996.

Yu, M. H., Wei, H. Y., Liang, Y., & Zhao, Y. (2013). Investigation of non-cohesive levee breach by overtopping flow. *Hydrodynamics, Ser. B, 25*(4), 572-579.

Yuan, S., Li, L., Amini, F., & Tang, H. (2015). Sensitivity of combined turbulent wave overtopping and storm surge overflow response to variations in levee geometry. *Journal of Coastal Research, 31*(3), 702-713.

Zhang, J. Y., Li, Y., Xuan, G. X., Wang, X. G., & Li, J. (2009). Overtopping breaching of cohesive homogeneous earth dam with different cohesive strence. *Sci. China Ser. E., 52*, 3024-3029.

Zhao, G. (2016). Breach growth in cohesive embankments due to overtopping. *Delft Academic Press*, 129-136.

Zhu, C. H. (n.d.). Breach growth in clay-dikes. *PhD Thesis, Delft University of Technology*. Delft, The Netherlands.

Zhu, Y. H., Visser, P. J., Vrijling, J. K., & Wang, G. Q. (2011). Experimental inverstigation on breaching of embankments. *Sci. China Ser. E., 54*, 148-155.